JOURNAL OF SPACECRAFT AND ROCKETS
Vol. 48, No. 3, May–June 2011

Effects of Control Power and Inceptor Sensitivity on Lunar Lander Handling Qualities

Eric Mueller,* Karl D. Bilimoria,† and Chad Frost‡
NASA Ames Research Center, Moffett Field, California 94035

DOI: 10.2514/1.49276

A piloted simulation studied the handling qualities for a precision lunar-landing task from final approach to touchdown. A core model of NASA's Altair Lunar Lander was used to explore the design space around the nominal vehicle configuration; details of the control and propulsion systems not available for that vehicle were derived from Apollo Lunar Module data. The experiment was conducted on a large motion-base simulator. Eleven space shuttle and Apollo pilot astronauts and one test pilot served as evaluation pilots, providing Cooper–Harper ratings, task load index ratings, Bedford workload ratings, and qualitative comments. Following attitude guidance cues, the pilots evaluated control powers ranging from 1.1 to 4.3 deg/s², maximum rate commands from 3 to 20 deg/s (equivalent to a range of inceptor sensitivities), and two magnitudes of disturbance moments arising from propellant slosh. The handling qualities were found to be satisfactory for the highest control powers and low inceptor sensitivities, with reduced sensitivity both improving handling qualities and reducing propellant use for a given control power. Pilots tended to use low attitude rates regardless of the maximum rate available or control power. Propellant slosh degraded handling qualities approximately one Cooper–Harper rating.

Nomenclature

c_{LQ}	=	linear-quadratic shaping parameter
g_{lunar}	=	gravitational acceleration at lunar surface, ft/s²
h	=	height above lunar surface, ft
$\dot{h}$	=	time derivative of h, ft/s
$I_{()}$	=	moment of inertia, slug · ft²
K	=	disturbance moment feedback gain
k	=	parameter for tradeoff between propellant consumption and error settling time
M	=	moment about a single axis, ft · lbf
m	=	vehicle mass, slug
p	=	roll rate, deg/s
q	=	pitch rate, deg/s
r	=	yaw rate, deg/s
T	=	thrust of descent engine, lbf
t	=	time, s
T^o	=	value of T required for vertical force equilibrium, lbf
α	=	angular acceleration about a single axis, deg/s²
δ	=	displacement of rotation hand controller
θ	=	Euler pitch angle, deg
τ	=	time constant, s
ϕ	=	Euler roll angle, deg
ψ	=	Euler yaw angle, deg
ω	=	commanded angular rate

Subscripts

body	=	with respect to body axes
cmd	=	commanded value
D	=	down component
DB	=	deadband
DE	=	descent engine
slosh	=	arising from slosh model
E	=	east component
err	=	error value
flat	=	offset of inner switching curve from deadband value
HI	=	boundary of rate error for two-jet vs four-jet control
N	=	north component

Superscripts

max	=	maximum command
P	=	pitch axis
R	=	roll axis
ROD	=	rate of descent
Y	=	yaw axis
$*$	=	reference variable

Presented as Paper 2009-6407 at the AIAA SPACE 2009 Conference and Exposition, Pasadena, CA, 14–17 September 2009; received 8 February 2010; revision received 28 January 2011; accepted for publication 30 January 2011.

*Aerospace Engineer, Flight Trajectory Dynamics and Controls Branch, Mail Stop 210-10; Eric.Mueller@nasa.gov. Senior Member AIAA.

†Research Scientist, Flight Trajectory Dynamics and Controls Branch, Mail Stop 210-10; Karl.Bilimoria@nasa.gov. Associate Fellow AIAA.

‡Deputy, Autonomous Systems and Robotics, Intelligent Systems Division, Mail Stop 269-1; chad.r.frost@nasa.gov. Associate Fellow AIAA.

Introduction

HANDLING qualities (HQs) are those characteristics of a flight vehicle that govern the ease and precision with which a pilot is able to perform a flying task [1]. They are a manifestation of the interaction between various factors that influence pilot perception of how well a vehicle can be used to accomplish a desired mission. These factors include the stability and control characteristics of the bare vehicle, the control systems that enhance these characteristics, the inceptors (e.g., control column, stick, or throttle lever) used by the pilot to transmit control commands, the visual cues from cockpit windows, displays and instrumentation that provide flight information to the pilot, and other cues (e.g., aural and tactile) that assist the pilot in the execution of the flying task. The effects of these factors on HQs have been studied in aircraft for decades [2–4], and reference standards for the HQs of both fixed-wing aircraft [5] and rotary-wing aircraft [6] have been developed and are now in common use. Broadly speaking, these standards define a subset of the dynamics and control design space that provides good HQs for a given vehicle type and flying task. HQs are important because the ease and precision with which pilots can execute a task has a strong effect on performance, mission risk, and training costs. At this time, no reference standards exist for HQs of piloted spacecraft.

NASA's Apollo program in the 1960s extensively studied manual control of the lunar module (LM) during lunar landing, with principal

goals of establishing simulation requirements for both research and training, selecting response types for attitude control, and designing the control system for compatibility with the pilot's control inceptor sensitivity and attitude control jet firing characteristics. A wide variety of lunar-landing simulators were constructed, including ground-based fixed and moving designs, a gantry design (the Lunar Landing Research Facility), and two free-flight simulation vehicles: the Lunar Landing Research Vehicle (LLRV) and Training Vehicle (LLTV) [7,8]. The studies conducted on those simulators showed that the most important pilot cues for the final approach and landing tasks on the moon were visual, motion, and auditory, in that order [7,9]. It was found that only the free-flight vehicles, LLRV and LLTV, could couple adequate visual and motion cues with a realistic trajectory for this task [6,9], and that the most difficult aspect of the lunar-landing task for pilots to master was the use of larger roll and pitch angles under lunar gravity in comparison with Earth to get equivalent translational accelerations [9]. However, it was recognized that a full spectrum of simulators was required to fully understand the lunar-landing problem and the complex interaction between automated systems and the pilot [8].[§] The control response types, which determined vehicle state commands as a function of pilot inputs, that were evaluated in these early simulations were attitude command, attitude–rate command (RC), and attitude acceleration command, with RC being judged to have the best HQs for final approach and lunar landing [10–12]. The parameters most important for HQs for an RC system are, in decreasing order, the angular acceleration available from the reaction control system (RCS), referred to here as control power (CP), the sensitivity of the rotation command inceptor, which is related to the largest rate that may be commanded at full inceptor deflection, and the size of the attitude–rate deadband [7,12–14].

To briefly summarize the large body of work that relates these factors to HQs of the LM as measured on the Cooper scale [15], the absolute minimum allowable CP was 5 deg/s^2 [14], with an optimum around 10 to 14 deg/s^2 (given a maximum inceptor displacement of 10 deg) [10,14]. CP has an important effect on the range of satisfactory inceptor sensitivities: near the optimum of 12.5 deg/s^2, the sensitivity was satisfactory between about 8 and 45 deg/s, while for larger CPs, the upper end of that sensitivity rose to 55 deg/s or more [7,10,12]. A rate deadband under 0.5 deg/s was measured to be satisfactory for these CPs and sensitivities, with degraded HQs becoming significant above 2 deg/s [12]. The use of proportional RCS thrusters instead of on–off thrusters was studied and, all else being equal, on–off thrusters were shown to significantly improve HQs because they appeared to deliver higher CPs [10]. Further study showed that improved HQs might be obtained by reducing inceptor sensitivity for the same CP, and that pilots rarely provided inputs that resulted in vehicle angular rates above 5 deg/s, even when the maximum available rate was 20 deg/s or more [13]. Reduced sensitivity also had the effect of reducing RCS propellant consumption [14]. These parameter selections were all based on subjective ratings by pilots using the Cooper scale [7,10,12–14]; evaluations of the effects of inceptor sensitivity and CP on landing point accuracy are notably absent [13]. Also absent was any evaluation of the potential impact of propellant slosh on HQs, an effect that made the landing task more difficult during Apollo 11 and required the addition of propellant tank baffles with their attendant mass penalties on future missions [16].

The simulation reported in this paper extends Apollo HQs work to inform the design of a next-generation lunar lander. The goal of the paper is not to measure the HQs of a specific vehicle; instead, the information contained in this report could be used to select preliminary values of important design variables, and it should provide information for trade studies on how to efficiently meet HQ requirements. The specific contributions of this paper lie in the evaluation of much lower CPs (up to a factor of five lower) than were considered during the Apollo era, which would result in a lower mass RCS, and an examination of the degree to which inceptor sensitivity can mitigate the known degradation of HQs that comes from low CPs. Contributions also include an extension of these parameter studies to a precision landing guidance-following task that may be required during future lunar outpost missions (requirements that were not present in the Apollo program) and a preliminary investigation of the effects of propellant slosh. The existence of key differences between the Apollo vehicle and the vehicle tested in this study (including different masses, CPs, tasks, and piloting cues) means that direct comparisons of results must be done with caution.

Finally, and not least of all, this study builds experience with the use of a high motion-fidelity ground-based simulator capable of providing the pilot with the most important cues identified by the Apollo studies (visual, motion, and auditory) in a much safer environment than the LLTV, which was prone to catastrophic crashes in moderate wind conditions. While some sort of free-flying simulator vehicle will undoubtedly be needed for training, the initial design work could be done in the safety of a ground-based simulator. This study continues the work of a recent simulation experiment in the same facility that demonstrated guidance cues are necessary for the manual execution of a precision landing using an Apollo LM design [17]. In this experiment, the vehicle design is updated with the mass properties, geometry, and propulsion system (both RCS and descent engine) specifications to match that of a preliminary NASA lunar lander design, the Altair vehicle (design and analysis cycle 2); the displays, inceptors, visual cues, guidance algorithms, and control algorithms were all designed independently from Altair. The RCS jet thrust was varied to achieve several different CPs that, along with the inceptor sensitivity (equivalently, the maximum RC, or max-RC), provided the experimental variables for the evaluation.

The paper begins with a discussion of the experiment design, which includes details on the flying task, test matrix, and procedure. A description of the vehicle design follows, where the lunar lander dynamics and control models are detailed. The ground-based motion simulator is described next, along with the cockpit instrumentation and piloting procedures. Results are then presented and, where applicable, given in the context of those obtained by Apollo studies. The paper concludes with a summary of key findings.

Experiment Design

A piloted simulation in December 2008 assessed the HQs for a precision lunar-landing task from terminal descent to touchdown. The primary experiment variables were the RCS jet thrust and RC at maximum deflection of the rotational hand controller (RHC), which are essentially the vehicle's achievable angular acceleration (or CP) and the inceptor sensitivity, respectively. The variables will be referred to as CP and max-RC. These variables had the most significant impact on HQs during the Apollo design process, and so they are good candidates for a preliminary HQ evaluation [13]. While the CP must be selected early in the design process and is difficult to change because of mass implications, the max-RC is controlled in software and can be changed easily to help mitigate the deficiencies known to result from low thrust levels. The magnitude of the rate deadband was found to have a crucial impact on HQs during the Apollo-era studies because it set the rate at which the vehicle could drift about each axis; that variable was not included in this study because an active attitude-hold feature eliminated residual drift when zero rate was commanded. The magnitude of the propellant slosh disturbance moment as a function of vehicle angular acceleration was a tertiary experiment variable; it was evaluated here for the first time for a lunar-landing task. The following sections describe various aspects of the experiment design.

Flying Task

The vehicle requirements for this simulation were derived from NASA's 2008 DAC-2 Altair model. The lander was to carry four astronauts, rather than the LM's two, and have stricter safety, precision, and performance targets, but it would be tasked with essentially the same mission: bringing people and cargo from lunar orbit to the surface and returning to orbit in an ascent stage that is separable from the lower portion of the lander. This experiment

[§]Data available at http://ser.sese.asu.edu/GO/GoReportVersion1.13.pdf [retrieved Sept. 2008].

evaluated HQs for a precision landing task, from final approach through terminal descent to touchdown, following a trajectory similar to the nominal Apollo trajectory. Coarse trajectory changes were made by firing opposing RCS jets to change the attitude of the lander and correspondingly tilt the descent engine's thrust vector. In a near-level attitude, fine trajectory changes in the horizontal plane could be made by firing several RCS jets in the same direction. Feedback guidance laws were developed for flying the precision landing task, and the corresponding guidance cues were displayed to the pilot via cockpit instrumentation. Details of the dynamics and control model are presented in the next section.

The task began at 500 ft (152.4 m) altitude with a forward speed of 60 ft/s (18.3 m/s) and a descent rate of 16 ft/s (4.9 m/s); for Apollo missions, this was known as low gate and represented the point on the trajectory where the manual flying phase would begin [18]. At this point, the spacecraft was 1350 ft (411.5 m) uprange from the designated touchdown point and pitched up 16 deg. The desired trajectory brought the spacecraft to a level attitude directly above the touchdown point, at an altitude of 150 ft (45.7 m), with a descent rate of 3 ft/s (0.9 m/s). This rate of descent (ROD) was held constant until one of the 6 ft (1.8 m) probes attached to the lander legs made contact with the lunar surface. A shutoff command was then sent to the main engine automatically, and the vehicle dropped until the legs settled on the lunar surface (in the Apollo LM, the pilots shut down the engine manually). This reference trajectory profile is illustrated in Fig. 1. For comparison, it also shows the uncontrolled trajectory that would result if no pilot inputs were made, starting from an initial condition with vertical force equilibrium.

The dynamics of the trajectory described previously are confined to the vertical plane, with pitch attitude as the primary means of longitudinal trajectory control. To excite lateral dynamics, the initial condition included a lateral offset of 250 ft (76.2 m) from the touchdown point, so that the initial velocity vector did not point directly at the landing site. This lateral offset required the pilot to use roll attitude as a means of lateral trajectory control.

Experiment Matrix

The experiment matrix was selected to bracket the Apollo LM and preliminary Altair CPs and a reasonable range of max-RCs. The average angular acceleration that is achievable across the roll and pitch axes for current RCS designs and mass properties is approximately 1.6 deg/s^2, and the low CP mode of Apollo, used when attitude or attitude–rate errors were small, was 4.3 deg/s^2. A CP intermediate between these was also tested, along with an even lower CP. While lower CPs tend to degrade HQs, it is important to know at what level of CP the task can no longer be accomplished with minimal workload, as that is the level likely to be implemented. This border of acceptable HQs is also important to map, because less costly system trades like display enhancements may compensate for the low CP. The CP was scaled in this experiment by directly changing the thrust level of the individual RCS jets. The values of max-RC also ranged from that of the Apollo LM, 20 deg/s, down to a low value that is close to the typical maximum rates actually used by pilots in earlier studies, 3 deg/s [13]. The preceding ranges were selected in consultation with a development pilot, a former space shuttle commander, to ensure a range of HQs ratings were received across the experiment matrix. This pilot did not contribute to data collection.

Two values of propellant slosh disturbance moment, the particular dynamics of which are given in the following section, were presented to the pilots. These conditions were always presented at the same levels of CP and max-RC, levels that were selected to correspond with a reasonable estimate of next-generation lunar lander values. Each pilot was presented with a random order of configurations and was not told what configuration he was flying in order to avoid biasing his ratings; however, in order to avoid learning-curve effects contaminating the results of the propellant slosh investigation, those two configurations were never presented as one of a pilot's first four configurations. The presence or absence of slosh was also blind to the pilots. The 18 configurations of the experiment (16 primary and two slosh) are shown in Table 1.

Evaluation Pilots

Twelve highly trained test pilots, including eight Shuttle pilot astronauts, three Apollo LM pilots, and one NASA test pilot, served as evaluation pilots, providing Cooper–Harper ratings (CHRs) [4], task load index (TLX) ratings [19], Bedford workload ratings [20], and qualitative comments. All pilots were male and had substantial training and experience as test pilots, logging an average of 6400 h on various fixed/rotary-wing and powered-lift aircraft and comprising 14 shuttle missions as pilot, nine as shuttle commander, and three Apollo missions. Each pilot was available to the experimenters for about 8 h, a constraint that determined the size of the experiment matrix.

Training Procedures

The pilots received a detailed briefing on the experiment background and objectives, flying task, control system, test matrix, and data collection procedures. Including discussion time, this session lasted approximately 1 h. This was followed by a 1 h motion-enabled training and familiarization session in the simulator cockpit, in which the pilot practiced the flying task for various CPs, max-RCs, and slosh magnitudes. This training was guided from within the cab by one of the experimenters, and piloting strategies designed by the development pilot were offered, but it was emphasized that the pilots should develop a strategy with which they were comfortable. Training continued until the pilot could achieve the desired performance parameters (listed in the next section), and they felt their learning curve was starting to plateau.

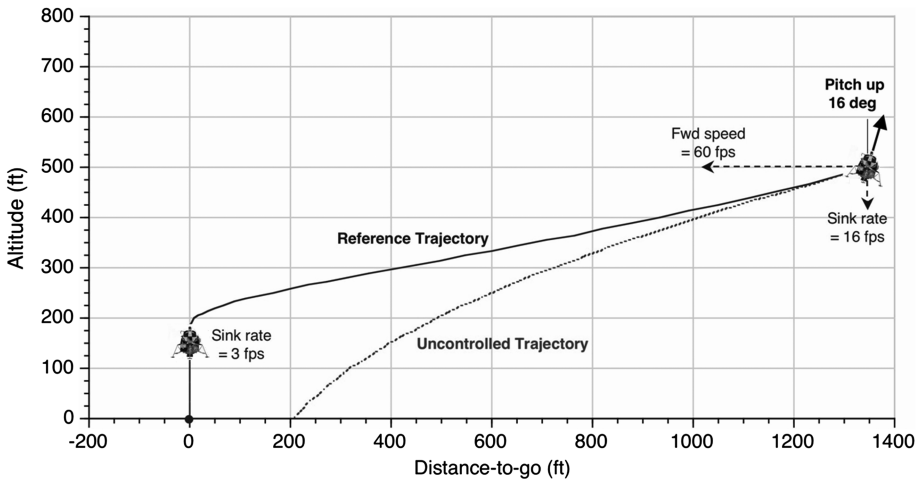

Fig. 1 Reference trajectory profile in the vertical plane.

Table 1 Experiment matrix

	CP			
Maximum RC	1.1 deg/s^2	1.6 deg/s^2	2.9 deg/s^2	4.3 deg/s^2
3 deg/s				
7 deg/s		Propellant slosh (2)		
12 deg/s				
20 deg/s				

Table 2 Limits of desired/adequate touchdown performance

Touchdown parameter	Desired	Adequate
Range to target point, ft	15	25
Horizontal velocity, ft/s	2	4
Descent rate, ft/s	6.5	8
Descent engine propellant burn, lbm	2060	2800
	35% remaining	10% remaining
RCS propellant burn, lbm	290	400
	35% remaining	10% remaining
Roll angle, deg	3	6
Pitch angle, deg	3	6
Roll rate, deg/s	3	6
Pitch rate, deg/s	3	6
Yaw rate, deg/s	1	1.5

Data Collection Procedures

Pilots flew all 18 configurations of the experiment matrix in random order, subject to the exception for slosh configurations discussed in the previous section. For each test configuration (e.g., CP of 4.3 deg/s^2 and 20 deg/s max-RC), the pilot flew a minimum of two consecutive data collection runs, with the option for as many additional runs as desired, and then provided experiment data for that test configuration as described next. Pilots flew the data collection runs in the simulator cab by themselves.

In HQs experiments, pilots are generally asked to make a composite assessment of the overall performance across all data collection runs for a test configuration. It is important to note that this assessment takes into account not just the quantitative evaluation of the endpoint (e.g., touchdown) performance but also a qualitative evaluation of the manner in which the vehicle gets to the endpoint. This overall assessment of desired, adequate, or inadequate performance is used for walking through the decision tree in the Cooper–Harper chart [1]. Pilots used the Cooper–Harper scale to assign HQ ratings from 1 (best) to 10 (worst) based on their assessment of task performance and effort. It is an ordinal scale, which means, for example, that the difference between ratings of 1 and 2 is not the same as the difference between ratings of 3 and 4. Ratings of 1, 2, and 3 on the Cooper–Harper scale correspond to level 1 HQs, which are a general requirement for normal operations of flight vehicles. Ratings of 4, 5, and 6 correspond to level 2, which may be acceptable for some offnominal conditions, and ratings of 7, 8, and 9 correspond to level 3, which is acceptable only for transition to a safe mode after a major failure/disturbance. Desired performance is necessary (but not sufficient) for level 1 ratings, and adequate performance is necessary (but not sufficient) for level 2 ratings. It is again noted that Apollo-era studies [7,9–14] on LM HQs used the Cooper rating scale [15], which was a precursor of the CHR scale used in this work.

At the end of each run, relevant touchdown performance parameters (see Table 2) were displayed to the pilot and experimenter; values outside the adequate performance bounds were color-coded red, those inside desired were green, and all in between were yellow. The values of desired and adequate performance bounds for key parameters were obtained from a survey of Apollo LM literature, with the primary consideration being confidence that adequate performance would not result in the vehicle tipping over or damage to the legs [21]; the 25 ft (4.6 m) range error limit for this precision landing task was obtained as approximately half of the diagonal distance between the Altair DAC-2 lander legs.

After making a composite assessment of the overall qualitative and quantitative performance across the data collection runs for a test configuration, pilots walked through the Bedford scale to assess their level of workload and available spare capacity (a quantity extrapolated by the pilot) in the task. Next, they assigned ratings for each of the six components of the NASA TLX [19]. These six components were physical demand, mental demand, temporal demand, performance, effort, and frustration. Finally, the pilots walked through the decision tree of the Cooper–Harper chart and assigned a HQ rating indicating the performance and level of pilot compensation required in that test configuration. As appropriate, pilots also made qualitative comments about the test configuration they had just evaluated. All pilot comments were recorded on electronic media; the experimenter noted key points.

A debrief session was held after all test configurations had been evaluated. The pilots were asked to fill out a one-page questionnaire designed to elicit high-level comments on cockpit displays, out-the-window displays, guidance cues, control response, and experiment design, along with a questionnaire that assessed the relative importance of the six TLX categories that would later be used to create a single weighted average TLX workload rating. The pilot's participation in the study concluded with a discussion of key insights and suggestions for future work.

Lunar Lander Dynamics and Control Model

NASA's Altair vehicle [22] was in the early design stages when model development for this simulation was finalized in November 2008, so the model is based only on available propulsion system characteristics, mass properties, and geometry of the vehicle. Some of the remaining aspects of the model, including control system design and switching curve logic, approach trajectory, and touchdown performance requirements, were based on Apollo LM data from several sources [13,23,24], and the remaining aspects, including displays, inceptors, and RCS prioritization logic, were designed specifically for this simulation. In the model used for this work, the lunar lander body axes system was a conventional aircraftlike system with origin at the center of mass (c.m.); see schematic in Fig. 2.

Vehicle Mass/Inertia Model

The initial mass of the vehicle when manual control begins is 1736 slugs (25,412 kg); it then varies due to consumption of propellant by the descent engine and RCS jets. During the final approach to touchdown phase, the vehicle mass decreases by only

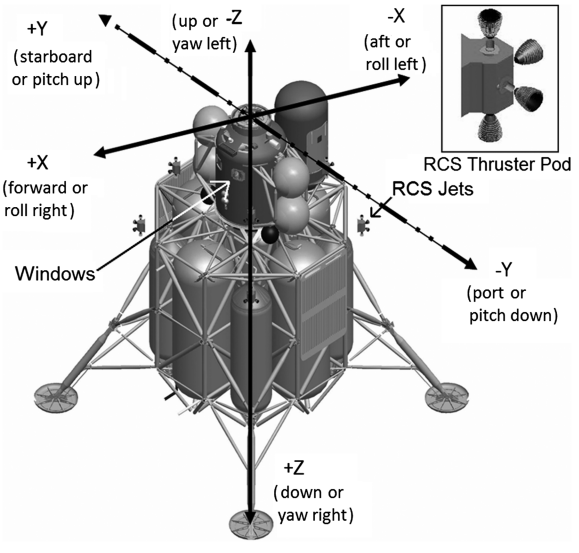

Fig. 2 Schematic of lander design.

5% due to propellant consumption; so in this model, the moments of inertia are constant and the vehicle c.m. location remains constant.

Descent Engine

The descent engine is the spacecraft's main rocket engine, with a specific impulse of 449 s. For the landing task, its thrust force is used to regulate the descent rate and to apply coarse trajectory control in the horizontal plane by rolling and pitching the vehicle. In this model, the engine does not gimbal, and the thrust line passes through the vehicle c.m. This assumption is an important condition of the HQ results presented here, because even minor thrust misalignments can severely limit the control authority about a particular axis or overwhelm the RCS entirely [14]. Propellant mass budgeted for the piloted segment of the landing trajectory is 98.4 slugs (1440 kg), which leaves about 70 s of propellant if the trajectory is flown perfectly.

The descent engine thrust is directed along the negative body z axis. During the flight phases from approach to touchdown, this thrust can be controlled by a throttle between 10 and 100% of the maximum value of 18,627 lbf (83,060 N). The thrust command T_{cmd} consists of two parts: T^o_{cmd} and ΔT_{cmd}. T^o_{cmd} is automatically computed as the force for which the vertical component balances the vehicle's lunar weight mg_{lunar} while compensating for vehicle roll and pitch angles:

$$T^o_{\text{cmd}} = \frac{mg_{\text{lunar}}}{\cos\phi\cos\theta} \tag{1}$$

The secondary part of the thrust command ΔT_{cmd} is an increment derived from pilot input. There are two modes for pilot input: a throttle-increment mode and a ROD mode. In the throttle-increment mode, each inceptor discrete input (click) by the pilot increments the thrust by $\pm 1\%$ of the upper throttle limit value of 18,627 lbf. In ROD mode, each inceptor click increments the commanded descent rate by ± 1 ft/s (0.3 m/s); the descent rate is regulated within a deadband of ± 0.1 ft/s (0.3 m/s) by a proportional feedback controller with a time constant $\tau = 1.5$ s:

$$\Delta T^{\text{ROD}}_{\text{cmd}} = \frac{m}{\cos\phi\cos\theta}\left(\frac{\dot{h}_{\text{cmd}} - \dot{h}}{\tau}\right) \tag{2}$$

Engine response to thrust commands is modeled as a first-order system, with a time constant of 0.11 s. Hence, the actual thrust produced by the descent engine T_{DE} lags the commanded thrust $T_{\text{cmd}} = T^o_{\text{cmd}} + \Delta T_{\text{cmd}}$.

Reaction Control System Jets

There are four RCS pods on the descent module, each of which has four RCS jets with thrust axes oriented along the vehicle positive and negative z-body axis and at 45 deg from the x and y axes in the x-y body plane. The c.m. of the vehicle at touchdown lies within the plane of the RCS pods, so no translation-into-rotation or rotation-into-translation coupling occurs because of offset thrust vectors (the nonzero value of I_{xz} term does cause a small amount of coupling between the x- and z-rotational axes). The RCS jets cannot be throttled and have fast response dynamics on the order of 10 ms. In this model, which is based on a generic on–off thruster, the response to a command input experiences a pure delay of 10 ms followed by a first-order thrust response that reaches full thrust within an additional 13 ms. The RCS jet must then fire for a minimum of 40 ms, after which the thrust decays as a first-order response with time constant 110 ms. Propellant mass budgeted for the piloted segment of the landing trajectory, including reserves, is 13.8 slugs (202 kg). RCS jets are used for three-axis attitude control; for the precision landing task, RCS jets can also be used for direct translation control in the horizontal plane when the vehicle is in a near-level attitude.

The firing logic design allowed any combination of simultaneous attitude and translation commands, whether from the pilot or the automated attitude control system. The price paid for this capability is a reduction in CP along all axes when commands are received about more than one axis. The CPs tested in this experiment, and shown in Table 1, represent the angular acceleration achievable when only a single-axis maneuver is being made. The layout and thrust directions of the RCS jets naturally separate the axes into two groups that do not compete with each other for individual jets. The $\pm z$ jets fire only for pitch and roll commands, so simultaneous rate commands for both those axes will result in half the expected angular acceleration in each axis. Similarly, the jets that lie in the x-y plane fire to meet yaw commands along with x and y translation commands, and the particular combination of commands received determines the factor by with the CP is reduced. Note that the z-axis jets are never fired for z translation because the descent engine controls that thrust axis, leaving pitch and roll commands to compete only with each other.

The RCS logic implemented in this experiment included an Apollo feature that reduced the number of jets used to create a moment when the attitude–rate error dropped below a threshold of 1.6 deg/s (using only two rather than four jets). Under these conditions, simultaneous roll and pitch commands would not reduce the angular acceleration from that requested by the control logic. The implementation of this feature within the attitude-hold logic will be described in a subsequent section.

Direct Translation Control

Pilot inputs are made with a three-axis translation hand controller (THC); this control inceptor is used for fine control of the trajectory along the x and y body axes when the vehicle is in a near-level attitude. The control response type is acceleration command; this means that the appropriate RCS jets fire continuously to produce a constant acceleration for as long as the pilot holds the inceptor out of detent. When the inceptor is in detent, the lander remains at nearly constant velocity, with accelerations resulting only from the tilting of the descent engine thrust vector because of small attitude dispersions within the attitude control system deadband.

Attitude Control

By tilting the descent engine thrust vector, roll/pitch attitude control provides indirect translation control for coarse trajectory changes. Pilot inputs are made with a three-axis RHC. This control inceptor is used for attitude stabilization and control along all three body axes; however, mode control is determined simultaneously for the roll and pitch axes (they are always in the same mode) and independently for the yaw axis. The yaw axis is treated differently, because it is not used for horizontal trajectory control, whereas the roll and pitch angles combine to affect the lateral and longitudinal vehicle accelerations. The attitude control response type is derived from Apollo and is described as a direct rate/pseudoautomode, implemented as described next and, in more detail, in [13].

Direct Rate Command Mode

This mode is in effect when the rate command in a particular axis is changing very quickly (in response to urgent commands [13], which for Apollo was a change in rate command of 6 deg/s in 1 s), and the attitude rate error is outside a 0.3 deg/s deadband. Error signals are generated as the difference between the actual and desired angular rates:

$$\begin{Bmatrix} p_{\text{err}} \\ q_{\text{err}} \\ r_{\text{err}} \end{Bmatrix} = \begin{Bmatrix} p - p_{\text{cmd}} \\ q - q_{\text{cmd}} \\ r - r_{\text{cmd}} \end{Bmatrix} \tag{3}$$

The commanded rates are computed from the inceptor deflection and the inceptor shaping function described in the following section. When the attitude–rate error is larger than 0.3 deg/s, the RCS firing logic is commanded to create a moment in the appropriate axis.

Pseudoauto Mode

A simple attitude-hold mode was implemented for all missions before Apollo 10: when the inceptor was in detent and the attitude–rate error was under 2 deg/s, the control system drove attitude and

attitude rate errors to zero using switching curve logic [13]. In all missions, beginning with Apollo 10, a hybrid mode was implemented to reduce attitude drift about uncommanded axes, provide more precise rate control, and improve HQs. This mode was in effect when both the commanded rate from the inceptor was changing slowly (e.g., less than 6 deg/s in 1 s for Apollo) and the rate error was within the 0.3 deg/s rate deadband. While this mode is active, the control logic integrates the commanded attitude rate (from the pilot's RHC) to obtain a commanded attitude. Then, both the attitude error and the attitude–rate error are used to look up moment commands based on phase–plane switching curves [24].

Error signals are given by

$$\begin{Bmatrix} p_{\text{err}} \\ q_{\text{err}} \\ r_{\text{err}} \end{Bmatrix} = \begin{Bmatrix} p \\ q \\ r \end{Bmatrix}$$

$$\begin{Bmatrix} \phi_{\text{err}} \\ \theta_{\text{err}} \\ \psi_{\text{err}} \end{Bmatrix} = \begin{bmatrix} 1 & 0 & -\sin\theta \\ 0 & \cos\phi & \sin\phi\cos\theta \\ 0 & -\sin\phi & \cos\phi\cos\theta \end{bmatrix} \begin{Bmatrix} \phi - \phi_{\text{cmd}} \\ \theta - \theta_{\text{cmd}} \\ \psi - \psi_{\text{cmd}} \end{Bmatrix} \tag{4}$$

where ϕ_{cmd}, θ_{cmd}, and ψ_{cmd} are equal to the sum of the Euler angle values captured when pseudoautomode was last entered (for the particular axis) plus the integral of the commanded rates. That is,

$$\phi_{\text{cmd}} = \phi(t_0^{R/P}) + \int_{t_0^{R/P}}^{t} p_{\text{cmd}}\,\mathrm{d} \qquad \theta_{\text{cmd}} = \theta(t_0^{R/P}) + \int_{t_0^{R/P}}^{t} q_{\text{cmd}}\,\mathrm{d}t$$

$$\psi_{\text{cmd}} = \psi(t_0^{Y}) + \int_{t_0^{Y}}^{t} r_{\text{cmd}}\,\mathrm{d}t \tag{5}$$

where $\phi(t_0^{R/P})$ and $\theta(t_0^{R/P})$ are the Euler roll and pitch angles captured when those axes last entered pseudoautomode, $\psi(t_0^{Y})$ is the yaw angle captured when that axis last entered pseudoautomode, and p_{cmd}, q_{cmd}, and r_{cmd} are the time-dependent attitude–rate commands from the RHC. Control moment commands are generated about the appropriate axes in accordance with the phase–plane relationship between error signals, as illustrated in Fig. 3 for the pitch axis. In Fig. 3, α_P is the nominal angular acceleration achieved with two RCS jets (half that shown in the experiment matrix; Table 1), $\theta_{\text{DB}} = 0.3$ deg is the deadband for pitch attitude error, $\theta_{\text{flat}} = 0.8$ deg is the magnitude of the flat boundary that enlarges the deadband region, $q_{\text{HI}} = 1.4$ deg/s is the rate error at which the control system transitions from two-jet to four-jet control, and $k = 0.01$ denotes the tradeoff between RCS jet propellant consumption and error settling time. The phase–plane relationships for the roll and yaw axes are identical, except for a small difference in the angular acceleration, α.

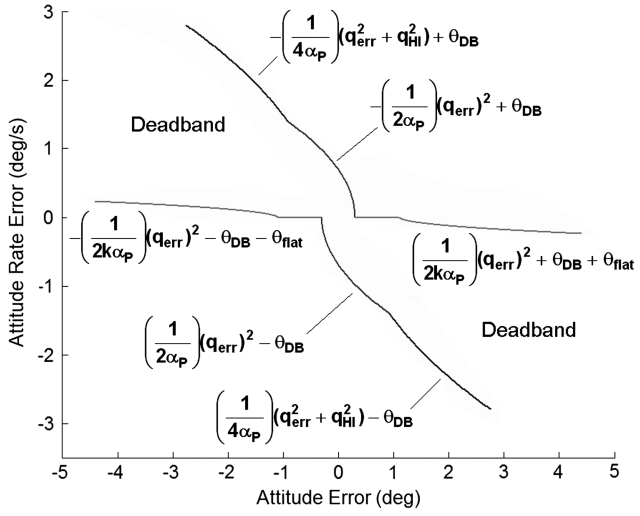

Fig. 3 Switching curves for pseudoautomode.

Guidance Laws

The Apollo lunar missions were required to land within several 100 feet of the designated landing site, an order of magnitude larger than would be required if touching down on a prepared pad. Therefore, the Apollo LM did not require, nor did it have, any active guidance cues displayed to the pilot for manual landing. The guidance laws used in this experiment were adopted without modification from an earlier lunar lander simulation, so only a brief description is given here, and the detailed derivation may be found in [17]. These laws were designed to guide the pilot along a reference trajectory (see Fig. 1) from final approach through terminal descent to lunar touchdown.

The guidance laws use the range to the touchdown point as the independent variable. First, the altitude rate is calculated according to the current altitude:

$$\dot{h}^* = (-0.03714h^* + 2.57) \quad \text{for } h^* \geq 150 \tag{6a}$$

$$\dot{h}^* = -3 \quad \text{for } h^* < 150 \tag{6b}$$

Next, the reference trajectory altitude at a given range from the landing site is derived [17]:

$$h^* = 69.2 + \left(\frac{80.8^{(\ell_n \sqrt{R/1350})}}{430.8}\right)^{1/[(\ell_n \sqrt{R/1350})-1]} \tag{7}$$

The vertical speed guidance is calculated next according to this reference altitude, which enables computation of the required horizontal velocity components as a function of range:

$$\dot{h}^G = (-0.03714h^* + 2.57) + \left(\frac{h^* - h}{\tau}\right) \tag{8}$$

$$V^*_{\text{horiz}} = 0.04444R[1 - 0.5\,\ell_n(R/1350)] \tag{9}$$

where $\tau = 25$ s. Finally, the guidance roll and pitch angles are calculated to provide the required horizontal acceleration components:

$$a_N^G = \left\{\frac{V_N V_N^*}{x} + \left(\frac{0.02222x\dot{R}}{R}\right)\right\} + \left(\frac{V_N^* - V_N}{\tau}\right) \tag{10a}$$

$$a_E^G = \left\{\frac{V_E V_E^*}{y} + \left(\frac{0.02222y\dot{R}}{R}\right)\right\} + \left(\frac{V_E^* - V_E}{\tau}\right) \tag{10b}$$

$$\phi^G = \sin^{-1}\left\{\frac{-m}{T}(a_N^G \sin\psi - a_E^G \cos\psi)\right\} \tag{11a}$$

$$\theta^G = \sin^{-1}\left\{\frac{-m}{T\cos\phi G}(a_N^G \cos\psi + a_E^G \sin\psi)\right\} \tag{11b}$$

Guidance cues are presented to the pilot as errors from the desired vehicle states. These errors are computed as the differences between the guidance and actual values of the roll/pitch angle and the differences between guidance and actual velocity components along the vehicle body axes. Details on the display of these guidance cues are presented in the next section.

Propellant Slosh Model

While a large body of work exists on the design of control systems to mitigate the effects of propellant slosh in unmanned space vehicles and in piloted aircraft, no design studies have yet investigated the effects of slosh on the HQs of a lunar lander vehicle, despite the known degradation that occurred during Apollo 11. The study of propellant slosh effects was a secondary objective of this experiment. The investigation was necessarily rudimentary, because existing

models were often too computationally intensive for real-time use [25]. Models could also be dependent upon experimental determination of relevant model parameters [26] or simply not relevant to the lunar lander's tank geometry [27]. The modeling approach was to employ a proven architecture for slosh [27] and model the propellant as a second-order transfer function in which the parameters were derived from pendulum dynamics under lunar gravity. The natural frequency of the pendulum, calculated from a moment arm of 1.97 ft between the vehicle c.m. and the propellant slug, under lunar gravity (5.32 ft/s^2) is $\omega_n = 1.64$ rad/s. The damping ratio of 0.02 was selected to match the disturbance period (2 to 3 s) reported by the astronauts on Apollo 11. This resulted in a transfer function from the angular acceleration of the body in a particular axis $\dot{q}_{\text{body}}$ to the disturbance moment in that same axis M_{slosh}:

$$\frac{M_{\text{slosh}}(s)}{\dot{q}_{\text{body}}(s)} = -K\frac{1.67}{s^2 + 0.064s + 2.70} \tag{12}$$

The higher value of the gain parameter, $K = 1500$, was selected to match the 2 to 3 deg by which the Apollo 11 vehicle was disturbed outside of its attitude deadband by the sloshing propellant, and the low value was simply half of the high, $K = 750$. In all other configurations, the gain value was set to zero.

Inceptor Shaping

The attitude rates commanded by the RHC were calculated by shaping the raw displacement of the inceptor using a linear-quadratic function, the same shaping function used in Apollo. This function is simply a weighted average of a linear function and a quadratic function:

$$\omega_{\text{cmd}} = \omega_{\text{cmd}}^{\max}\left(\frac{(\delta - \delta_{\text{DB}}) + c_{\text{LQ}}(\delta - \delta_{\text{DB}})^2}{(1 - \delta_{\text{DB}}) + c_{\text{LQ}}(1 - \delta_{\text{DB}})^2}\right)$$
$$\text{if } \delta > \delta_{\text{DB}}; \qquad \text{else } \omega_{\text{cmd}} = 0 \tag{13}$$

where ω_{cmd}^* denotes the angular rate commanded at full throw of the RHC ($\delta = 1$). The parameter values used in this experiment were $c_{\text{LQ}} = 10$, which is close to parabolic shaping, the RHC deadband was 10% of full throw, and ω_{cmd}^* varied depending on the configuration being tested.

Simulation Environment

The experiment was conducted in the vertical motion simulator (VMS) at NASA Ames Research Center. The VMS is a large motion-base simulator [28] that has been used for numerous HQs evaluations of aircraft and spacecraft [17,29,30]. Simulations have found that the most important pilot cues for the final approach and landing tasks on the moon were first visual, followed by motion, and then auditory [7,9]. Six-degree-of-freedom simulator motion was used for the experiment because the reference trajectory was dynamic, featuring significant translational accelerations (~3 ft/s^2) and roll/pitch angular motion (~15 deg).

The Apollo LM pilot stations had a standing configuration to improve downward visibility and reduce vehicle mass by eliminating seats. One of the VMS interchangeable cabs was structurally modified to provide a similar cockpit configuration, as illustrated in Fig. 4. The evaluation pilot occupied the left station; the right station was occupied by the experimenter during training runs but was unoccupied for data collection runs. Each pilot station provided a three-axis RHC and a three-axis THC mounted on the right and left armrests, respectively. A button on top of the RHC toggled between the descent engine control modes of throttle increment and descent rate. Up/down motion of the THC adjusted the commanded value of the throttle increment or ROD, depending on the selected mode.

A simulated view of the lunar landscape was projected on a set of five noncollimating flat-screen rear-projection color displays. The designated landing site was depicted by a 50-ft-diam (15.2-m-diam) red circle enclosed by a slightly larger red square on the lunar surface. The display had a large field of view: 77 deg vertical and 225 deg horizontal. Window masking was not used in the simulator cockpit; therefore, the entire field of view was available to the pilot. This is not representative of actual operations in which the pilots have only limited views of the lunar landscape through small windows. However, the precision landing task in this experiment was essentially a head-down task, and the pilot's attention was focused primarily on the cockpit instrumentation rather than the view outside the cockpit.

Cockpit Instrumentation

Cockpit displays were mounted on a console providing two 9 in. flat-panel monitors at each pilot station and a 15 in. flat-panel monitor in the center. The pilot station displays are shown in Fig. 5; the center monitor showed a camera view positioned 5 ft ahead of the descent engine nozzle and oriented along the $+z$ direction (downward facing). The displays were adapted from Apollo LM instruments where possible; otherwise, existing rotorcraft or glass cockpit aircraft displays were implemented.

The left display has a north-referenced moving map section, with a triangle in the center representing the spacecraft and the dark circle indicating the landing site. The rings indicate range from the spacecraft's current location, and the radial lines indicate bearing angles in increments of 30 deg. The map rescales (zooms in) as the spacecraft approaches the landing site. The diamonds on the map section indicate the body x- and y-axes components of the vehicle's speed (in feet per second). The bars on the map section are speed error needles that provide guidance for the vehicle's longitudinal and lateral speeds. This guidance is fly to, meaning that, given the scenario in Fig. 5, the pilot should move the THC backward and right to drive the error needles to zero. However, it is noted that THC inputs are effective only when the vehicle is in a near-level attitude in the vicinity of the landing site. Immediately below the moving map are digital readouts of range-to-go as well as its x (downrange) and y (crossrange) components in units of feet. Next to the map section are thrust indicators and gauges showing propellant mass available for the main descent engine and the RCS jets.

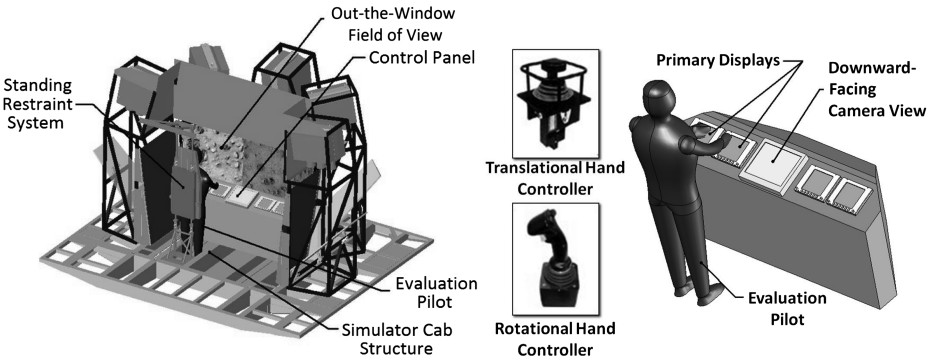

Fig. 4 Simulator cockpit layout.

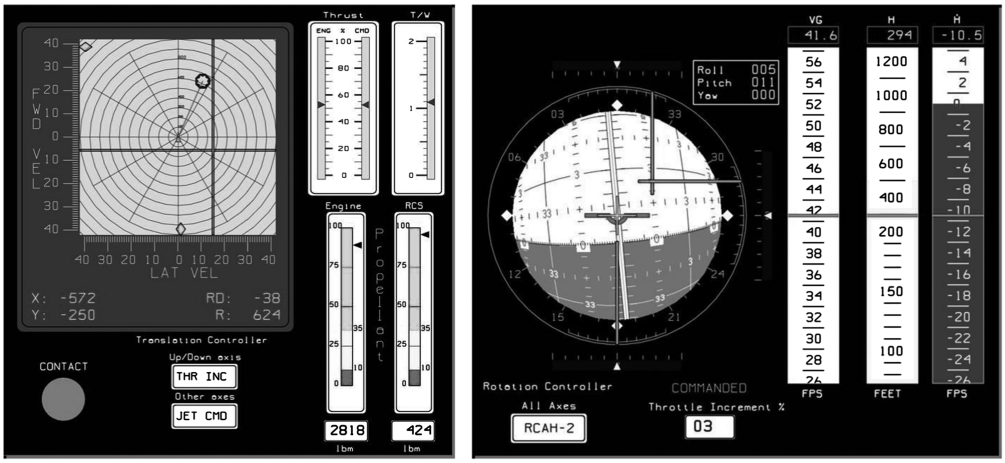

Fig. 5 Pilot station displays.

The right display shows an attitude director indicator (ADI) with a digital readout of the roll, pitch, and yaw angles. The small triangles on the scales around the ADI indicate the body roll, pitch, and yaw rates. Each tick mark on the scale is 5 deg/s. The cross-shaped symbol in the center of the ADI represents the direction of the lander's nose, and the horizontal and vertical bars referenced to the cross are attitude error needles providing guidance for roll, pitch, and yaw angles. This guidance is fly to, suggesting that the pilot use the RHC to roll right and pitch up to drive the error needles to zero. In the experiment, the yaw guidance was turned off and pilots were advised not to make any yaw-axis RHC inputs, because it added significant workload while adding little value to the flying task. However, the yaw attitude-hold function was always active to null any yaw disturbances. On the lower right of the ADI are annunciators for the throttle mode (throttle increment or descent rate) and the current commanded value for the selected mode. To the right of the ADI are three moving tape displays for horizontal speed (in feet per second), altitude (in feet) and altitude rate (in feet per second).

Piloting Technique

The following procedures were reviewed with each pilot during the initial briefing. The pilots practiced these procedures during the training and familiarization simulator session before data collection.

Vertical Speed Control

Vertical speed control is accomplished by throttling the descent engine, which in throttle-increment mode is done manually by incrementing the THC up or down to change the thrust by 1% of the maximum. The simulation task began in throttle-increment mode with a ΔT_{cmd} setting of 3%. This had the effect of reducing the descent rate from an initial value of 16 ft/s at 500 ft altitude to 3 ft/s at approximately 150 ft altitude in the vicinity of the landing site. Pilots were advised to switch to ROD mode (by pressing a button on top of the RHC) at this point and, if necessary, adjust the descent rate to 3 ft/s with up or down inputs from the THC.

Horizontal Speed Control

Horizontal speed control is accomplished by rolling and/or pitching the vehicle to tilt the descent engine thrust vector. Pilots were advised to follow guidance commands by first using the RHC to null the roll/pitch angle error needles on the ADI until the vehicle reached a near-level attitude in the vicinity of the landing site and then using the THC to null the local horizontal speed error needles on the map display until touchdown. However, it was possible to fly the vehicle all the way to touchdown using only the RHC by following the guidance error needles on the ADI.

Motion Cueing

Providing realistic motion cues for this task at first appears to be a challenge because the VMS operates in the Earth's gravity field, which is about six times stronger than that of the moon. However, the goal of motion simulation is simply to approximate the translational and rotational accelerations at the pilot station. A 1 ft/s^2 longitudinal/lateral acceleration or a 1 deg/s^2 roll/pitch/yaw acceleration is experienced by pilots in the same way, regardless of the gravity field in which the vehicle is flying. The vertical acceleration due to lunar gravity cannot be provided by an Earth-based simulator because it requires a constant large vertical acceleration of the simulator cab, but incremental vertical accelerations relative to lunar gravity can be approximated in a manner similar to the longitudinal/lateral accelerations. The motion program of the VMS initially simulates the accelerations calculated at the lunar lander pilot station and then attenuates the accelerations so that the simulator cab does not reach its physical travel limits. The movement of the out-the-window visual scene in the simulator cab continuously matches the calculated lunar lander motion states, thereby creating the illusion of persistent motion.

Results

Data collection was conducted with 12 pilots between 8 December 2008 and 19 December 2008, and again between 26 January 2009 and 30 January 2009. The subjective HQ ratings given by the pilots included CHRs, NASA TLX ratings, and Bedford workload scale ratings, although only results from the first two scales will be presented here; the Bedford ratings did not contribute additional insight into the task, as reported previously [31]. Objective data were captured during the simulation on the touchdown range dispersions, RCS propellant usage, and the distribution of commanded versus actual attitude rates. These data were all collected with propellant slosh on and off.

Handling Qualities Ratings

The CHRs provided by the 12 pilots for each of the 16 combinations of the primary experiment variables are shown in stacked bar chart form in Fig. 6. The shades of gray in that figure represent HQ levels 1, 2, and 3 (corresponding to CHRs 1–3, 4–6, and 7–9, respectively), where lighter shades are better ratings. The black block in the 1.6 deg/s^2, 20 deg/s configuration represents two ratings of 10, also referred to as level 3+, meaning that the pilot felt control would be lost in that configuration. Configurations are first grouped by the CP and then are subdivided by the max-RC. All pilots were able to rate all configurations of this experiment matrix.

Figure 6 shows that HQs improve with higher CPs (RCS jet thrust levels), up to at least those tested in this experiment, for any given max-RC. That is, for a given max-RC, the HQs improve as CP

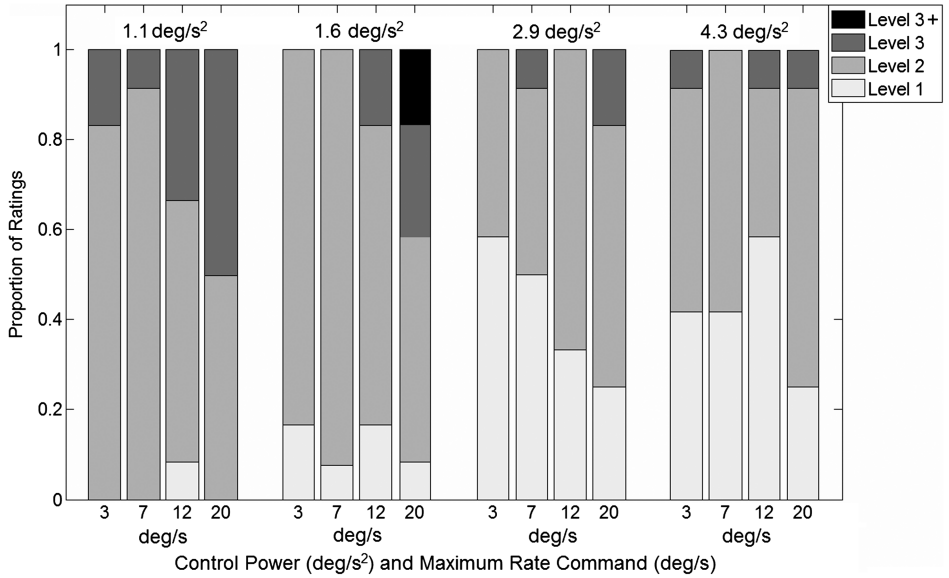

Fig. 6 Proportion of HQ levels for the 16 primary configurations.

increases. This fact is consistent with the results of HQ evaluations with aircraft: the faster the vehicle responds to pilot inputs, the better the HQs, as long as the response is not so fast that the pilot cannot make precise maneuvers. The improvement is less distinct between the two highest CPs, suggesting that little is gained from a HQ perspective by increasing the achievable angular acceleration from 2.9 to 4.3 deg/s^2.

Another result from Fig. 6 is that variations in the max-RC have a smaller effect at high CPs than at low ones, and that, in general, the lowest max-RC value is rated best. This trend is more easily distinguished by looking only at the median values of CHR, which are shown in Fig. 7. Overall, the 20 deg/s max-RC was rated worst for any value of CP, but at the two higher thrust levels, the spread in the median ratings was only 0.5 to 1. While this is not insignificant (and it would be valuable information to a designer interested in a software quick fix for a HQs deficiency), it is much smaller than the 1.5- to 2-point improvement that max-RC can deliver at the lower CPs (e.g., from a six to a four at 1.6 deg/s^2). The important result of Figs. 6 and 7 is that if one must design a lunar lander with a CP of 3 deg/s^2 or lower, then the lower the max-RC the better, at least down to 3 deg/s. In fact, the HQs can be improved by a full rating point or more simply by using this lowest value of rate command. At the highest CP, the 12 deg/s max-RC seems to be the preferred configuration, a result that matches the Apollo-era result at much higher CPs, but the preference is not strong, and other max-RCs get almost as many level 1 ratings. It is also important to reiterate that the Apollo LM max-RC of 20 deg/s is too high from a HQs perspective and, if pilots insist on having such a rate available for emergency situations, a selectable rate system like that available on the space shuttle orbiter [32] should be used rather than a fixed value that is not optimal.

Another approach to showing the relationship between HQs and the parameters tested in this experiment is by cross plotting the median CHR against max-RC and CP. These contour plots were used extensively in the Apollo studies to identify the region in which HQs were level 1 and in which surrounding regions represented degraded HQs; such a chart was sometimes referred to as a thumbprint because of the nested contours denoting levels 1, 2, or 3. Figure 8 shows the median ratings with labeled contours of constant CHR between HQ levels; these contours are found by interpolating between ratings provided by the pilots. That plot suggests there may be an area of level 1, or at least borderline level 1/2, HQs for the higher CPs and correctly selected max-RCs. The granularity of the test configurations in this region makes it difficult to predict the precise shape of the level 1 region, but it does appear to exist for the precision landing with a guidance-following task within the range of experimental configurations tested.

The bottom right data point in Fig. 8 (i.e., corresponding to 20 deg/s and 1.1 deg/s^2) has a median rating of 6.5 and so probably represents the tip of a region of level 3 HQs. Pilots reported that the available max-RC and the CP were poorly matched, and that the vehicle response was excessively sluggish. Pilot-induced oscillations tended to occur at a maximum rate of 20 deg/s and at both 1.1 and 1.6 deg/s^2 CP because of this poor match, a factor that will be illustrated in the next section. One way to explain such

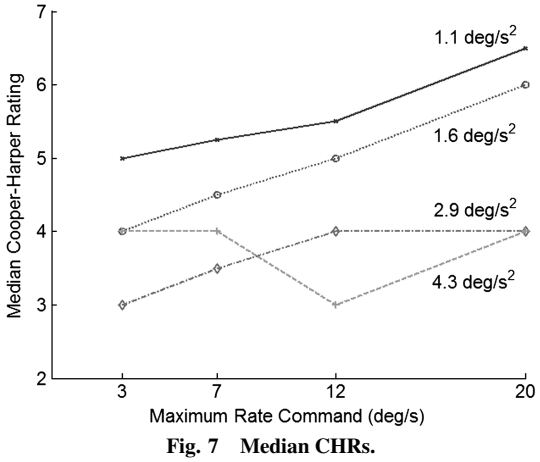

Fig. 7 Median CHRs.

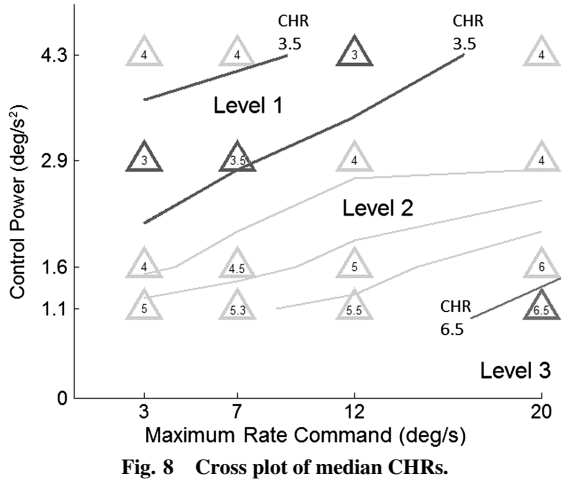

Fig. 8 Cross plot of median CHRs.

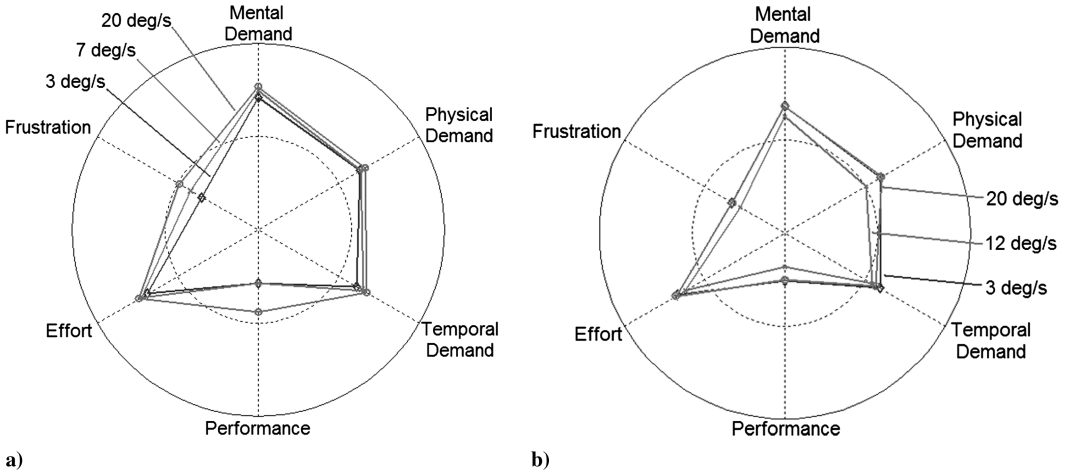

Fig. 9 NASA TLX ratings for a) 1.6 deg /s^2 and b) 4.3 deg /s^2.

degradation in HQs is by noting that, at the lowest CP, the vehicle would take more than 18 s to ramp up to the max-RC of 20 deg /s. This effectively makes the attitude response type a direct acceleration command rather than a rate command system, a configuration found to have poor HQs by Apollo studies.

HQ ratings appear to get worse in the upper left portion of Fig. 8 for two reasons: the CP is getting high enough that the vehicle response begins to feel jerky, and the max-RC is too low for the high CP and fast dynamics of the vehicle. The best HQs result from appropriate selection of max-RC given the CP, the diagonal region in the upper left of Fig. 8, and from relatively high CPs, as long as the vehicle response is not jarring.

Workload Ratings

The NASA TLX scale is intended for use in any task, whether a pilot-in-the-loop flying task, a checklist with a series of button pushes, or the manipulation of a robotic arm. The usefulness of the scale lies in the quantification of workload in six different categories, which allows the experimenter to determine what type of workload is contributing to the difficulty of the task and not simply how much total workload is involved. A drawback to the scale is large interrater variability due to the anchoring of the ends of the scales with only the adjectives high and low. This problem is mitigated to some extent by using the scale only to compare different configurations rated by the same participants and averaging all the ratings; as long as the intrarater variability is small, these comparisons are meaningful. Plots of the six workload factors for six configurations, 1.6 and 4.3 deg /s^2 paired with 3, 12, and 20 deg /s, are shown in Fig. 9 (the outer, solid circle represents maximum workload, while the inner, dotted line represents intermediate workload). In that figure, smaller numbers represent lower workload in a particular category, so smaller polygons represent less overall workload. The TLX results show some of the same trends as the CHR data: higher CPs require less work from the pilot to accomplish the task, and lower max-RCs also lower the workload to a point. The benefit of these lower maximum rates is greater in the lower CP case, where there is a monotonic decrease in workload in every category with decreasing maximum rate, reinforcing the conclusion that judicious selection of maximum rate can mitigate HQ deficiencies resulting from low CP. For example, with a CP of 1.6 deg /s^2, the best maximum rate is 3 deg /s, while a CP of 4.3 deg /s^2 achieves a minimum workload at 12 deg /s and there is little to distinguish 3 and 20 deg /s.

Pilot–Vehicle Performance

The range from the lander centerline to the center of the landing pad, termed the radial offset, was the primary variable the pilots were trying to control. HQ studies during the Apollo-era did not look at the touchdown performance or measure it as a function of the HQ parameters under investigation, but it was identified as an important metric with which to assess pilot–vehicle performance in the future [13]. A plot of the downrange and crossrange errors at touchdown as a function of configuration is shown in Fig. 10. Note that 4 of the 416 landings occurred well outside the adequate range, but they are not shown in Fig. 10 because the primary region of interest is within the adequate range. A trend that is difficult to discern in Fig. 10, but which is clearer in the plot of median radial offset in Fig. 11, is that the range tends to improve with higher CPs, but that the improvement is substantial only from the lowest to the next lowest value of CP. The improvement was expected because pilots could use the THC to fine-tune their landing accuracy at higher CPs. Yet, it was unexpected that 1.1 deg /s^2 would be so much worse than the other values of CP, or that 1.6, 2.9, and 4.3 deg /s^2 would all show approximately the same performance. It is not known why the low max-RCs at 2.9 deg /s^2 did so poorly in radial offset, but it could be due to chance, as the max-RC does not directly influence the pilot's ability to fine-tune the touchdown accuracy with the THC.

The RCS propellant used during the simulation runs as a function of configuration is shown in Fig. 12. This is an important metric, because reductions in propellant uses translate into mass savings, which is difficult to achieve in any but the earliest design cycles. Figure 12 uses box and whisker plots to show the range of the data, with the median being represented by the line inside the box, the first and third quartiles (25 and 75% of the data) being represented by the edges of the box, and the whiskers representing the total extent of the data not including outliers. (An outlier is defined as more than twice the interquartile range from the median.) The notches in the boxes represent 95% confidence intervals for the medians, and boxes without overlapping notches indicate statistically significant differences between the medians of those configurations (at the $p < 0.05$ level using analysis of variance). Propellant use goes down

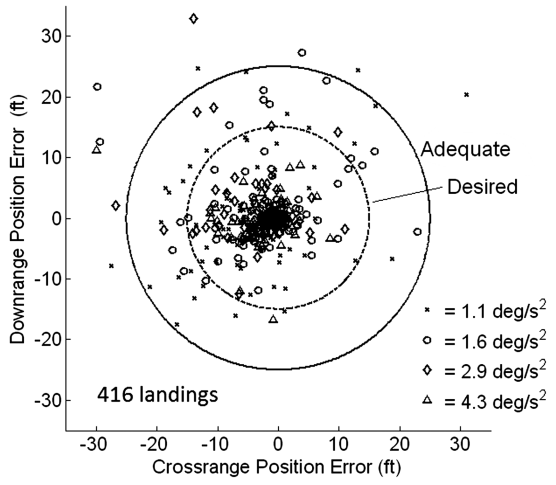

Fig. 10 Range to target point at touchdown.

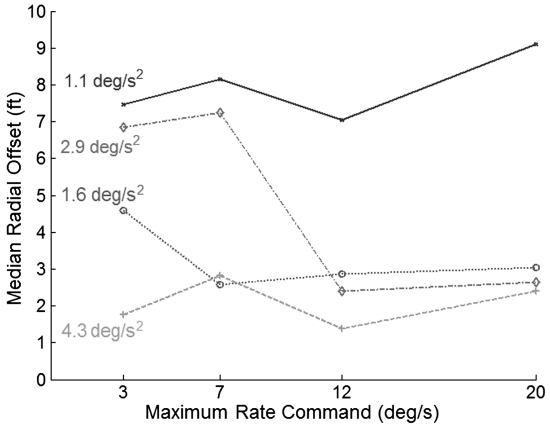

Fig. 11 Median range to target point at touchdown.

as the CP (equivalent to the RCS jet thrust) goes down, and it decreases as the max-RC goes down. These trends are monotonic with only one or two exceptions and, together with the CHR data, show that HQs and propellant use can be improved by reducing the max-RC. Unfortunately, the CP cannot be used to improve both metrics simultaneously; improved HQs for these variations came at the expense of additional propellant use.

Attitude Rates

In the Apollo studies, pilots preferred to use the smallest attitude rates they could reliably command, regardless of the maximum rate that could be commanded, and almost no rates above 6 deg/s were ever used in the simulations [13]. This result relates to CP in the sense that a pilot wants harmony between the rates that can be commanded (the max-RC) and the ability of the attitude control system to meet those rates in a timely manner (i.e., by having sufficiently high CP). One way to measure such harmony is by calculating the time required to reach 63% of the maximum rate in an analogy with the time constant of a first-order response; Apollo studies determined that a pilot would accept a time constant of no more than 5 s [10]. This study did not cast the experiment matrix in terms of the time constant, but in postanalysis, the relationship between the commanded and actual rates could be determined and conclusions could be drawn about the characteristics of a system exhibiting harmony between commanded and actual attitude rates. In the discussion that follows, only roll rate is analyzed. The roll rates were symmetric about zero because the task called for a roll right followed by a roll left. The pitch rates were significantly biased toward negative rates.

One way to indicate CP harmony with maximum commanded rate is by plotting the root-mean-square (rms) value of the actual and commanded rates. Because rms is a measure of the spread of data (it is equal to the standard deviation for a population with zero mean), it can be used to infer whether the rates being commanded by the pilot are actually being achieved. The plot in Fig. 13 shows the rms actual and commanded values as a function of configuration, and the most striking feature of the data is that the rms actual roll rate is essentially independent of either the CP or the maximum commanded rate: values vary between 0.8 and 1.1 deg/s. This confirms the Apollo result that pilots want to use the smallest rate possible to complete the task, and it again supports the recommendation that very low maximum rates should be provided to the pilot in a lunar lander design. There are no data to suggest high angular rates were ever achieved or would be useful in any circumstances, emergency or otherwise, because high rates and low CPs often lead to loss of control. Figure 13 also shows that some configurations that received poor HQ ratings (e.g., 1.1 and 3 deg/s) have good harmony, indicating that harmony may be a necessary but not sufficient condition for good HQs. Correlating the results in Fig. 13 with the ratings in Fig. 6 shows that, for a given CP, it is possible to improve HQs by careful selection of the max-RC for harmony, but that even harmony will not sufficiently address the problems experienced by pilots at low CPs.

Propellant Slosh

A secondary goal of this study was to conduct a preliminary investigation of the impact of propellant slosh on HQs for a single configuration (1.6 deg/s^2 and 7 deg/s). CHR data in Fig. 14 appear to confirm the hypothesis that disturbance moments degrade HQs; however, the trend is not a strong function of the disturbance magnitude. The median rating is the same when there is no slosh or a small amount of slosh, and the number of level 1 and level 3 ratings goes up with small disturbances. With the larger gain in the slosh transfer function, the median CHR does worsen by one point and there are no level 1 ratings, but the number of level 3 ratings does not increase. It should be repeated that the propellant slosh model was not high fidelity, and these results should not imply that propellant slosh will not be a problem for a lunar lander in this configuration (1.6 deg/s^2 and 7 deg/s). However, it does appear that the low angular accelerations achieved at this CP are not sufficient to excite the modeled propellant slosh frequencies. Informal testing at higher CPs seemed to indicate that slosh would be a bigger problem with more powerful RCS thrusters, so further testing with a detailed slosh model and lander characteristics closer to a final design will be warranted.

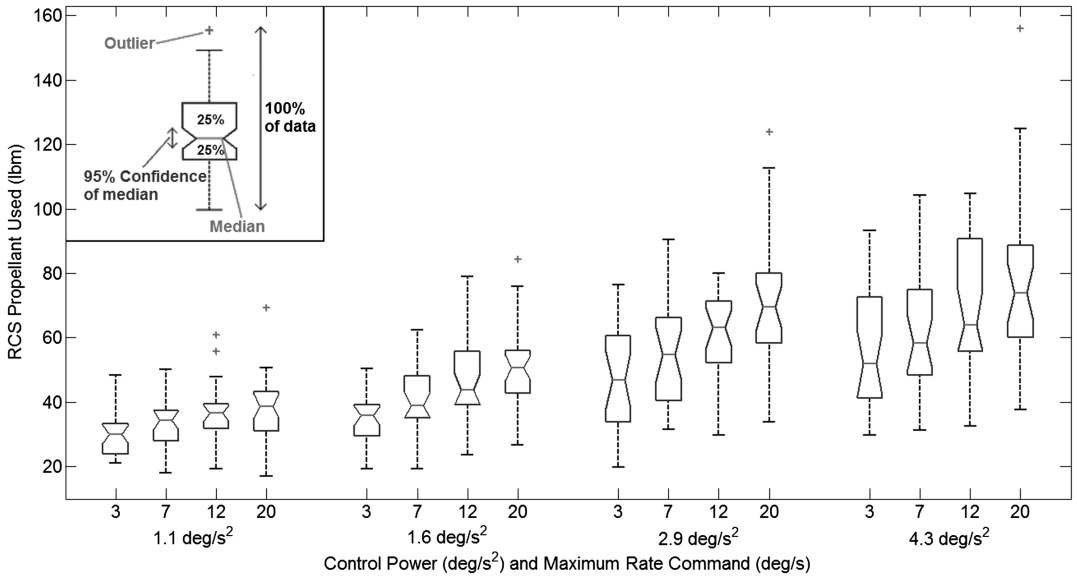

Fig. 12 RCS propellant used.

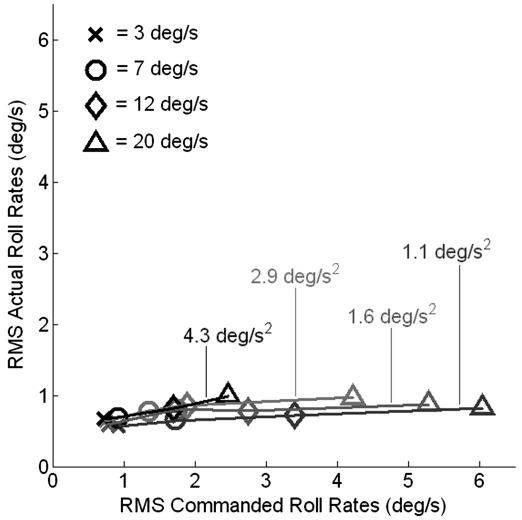

Fig. 13 RMS commanded and actual roll rates.

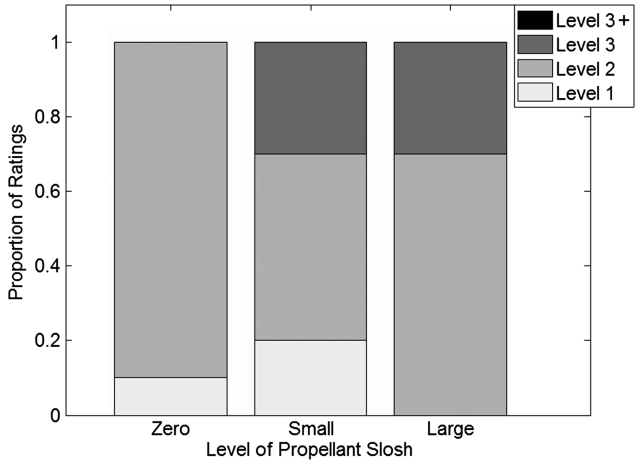

Fig. 14 Proportion of HQ levels with propellant slosh for 1.6 deg/s^2 and 7 deg/s.

Conclusions

Twelve NASA astronauts and test pilots participated in a simulation evaluation of the HQs of a lunar lander during the final phase of a precision approach and landing using attitude error guidance. The parameters under study were the CP, defined as the angular acceleration that could be achieved by the vehicle, and the angular rate commanded at maximum inceptor deflection, which is equivalent to inceptor sensitivity. A secondary objective was to measure the HQ degradation from propellant slosh. Altogether, 18 configurations were tested, with CPs ranging from 1.1 to 4.3 deg/s^2, max-RCs ranging from 3 to 20 deg/s (equivalent to a range of inceptor sensitivities), and two levels of propellant slosh.

HQs improve with increasing CP and decreasing max-RC, but the interplay of these two factors is not necessarily linear or monotonic. CPs around 2.9 deg/s^2 or higher appear to have similar HQs, up to the limit of the tested CP of 4.3 deg/s^2, and CP appears to be the dominant factor in comparison with max-RC. At these higher CPs, the HQs are borderline level 1/2, and at the lower CPs between 1.1 and 1.6 deg/s^2, the HQs range from level 2 to borderline level 2/3. CP alone was not sufficient to achieve level 1 for the guidance-following precision landing task, but it did improve range performance at touchdown and achieve better correspondence between the attitude rates the pilots commanded and the attitude rates that were actually achieved. For a precision lunar-landing task with attitude guidance, CP in the roll and pitch axes should be around 3 deg/s^2 at a minimum, and even higher if propellant consumption and mass will allow it.

The max-RC had an important effect on HQs at all but the highest CP, and in those cases, reducing the max-RC was shown to both improve HQs and reduce propellant consumption. For the highest CP, 4.3 deg/s^2, the maximum rate had little impact on HQs as long as it was 12 deg/s or less. For all lower CPs, the best HQs were achieved at 3 deg/s for maximum inceptor displacement (in some cases, even achieving level 1); this seemingly low value is consistent with the attitude rates achieved by the lander at the highest CPs and max-RCs, suggesting that higher maximum rates are not only unnecessary but also detrimental to pilot performance and/or workload. Low maximum rates contribute to good control harmony for the ranges of CP tested and reduce propellant consumption, but they did not have any effect on range at touchdown performance. The combined maximum rate and CP results have been used to estimate the boundaries of a region with level 1 HQs for a precision landing task following attitude guidance. The commanded attitude rate at maximum inceptor deflection should be between 3 and 7 deg/s unless a clear circumstance is identified in which a higher rate is necessary and that rate does not degrade HQs.

The propellant slosh results confirm that HQs degrade as the magnitude of the disturbance moment increases, but the net degradation was not large. Median CHRs were the same for the no-coupling and low-coupling cases, and they worsened by one point in high coupling. It is believed that the low value of CP under which slosh was tested contributed to the lack of a strong degradation in HQs, and that a vehicle with higher CP would experience poorer HQs than measured in this experiment.

Acknowledgments

The SimLabs staff at NASA Ames Research Center set up the details of the experiment on the vertical motion simulator, and their efforts are greatly appreciated. In particular, the authors would like to acknowledge the substantial contributions of simulation engineers, Mike Weinstein, Mike Leonard, and Scott Reardon, who developed and tested all software for the lunar lander dynamics and control model and assisted in day-to-day execution of the experiment. Karol Bobko served as project pilot and contributed to model development and testing, and both he and Kathleen Starmer recruited the outstanding pool of evaluation pilots. Boris Rabin created the out-the-window visuals. Thanks are also due to Kevin Duda, Michael Johnson, and Steve Pashcall from the Autonomous Landing and Hazard Avoidance Technology Project, Dougal MacLise and Ron Sostaric of the Altair Project, and Howard Law for providing Altair mass properties, dimensions, and propulsion system data.

References

[1] Cooper, G. E., and Harper, R. P., "The Use of Pilot Rating in the Evaluation of Aircraft Handling Qualities," NASA TN D-5153, April 1969.

[2] Soule, H. A., "Preliminary Investigation of the Flying Qualities of Airplanes," NACA Rept. 700, 1940.

[3] Gilruth, R. R., "Requirements for Satisfactory Flying Qualities of Airplanes," NACA TR 755, 1943.

[4] Cooper, G. E., and Harper, R. P., "Handling Qualities and Pilot Evaluation," *Journal of Guidance, Control, and Dynamics*, Vol. 9, No. 5, Sept.–Oct. 1986, pp. 515–529. doi:10.2514/3.20142

[5] "Flying Qualities of Piloted Airplanes," U.S. Department of Defense, MIL-STD-1797, Washington, D.C., March 1987.

[6] "Performance Specification: Handling Qualities Requirements for Military Rotorcraft," U.S. Army Aviation and Missile Command, ADS-33, Redstone Arsenal, AL, May 1996.

[7] Matranga, G. L., Mallick, D. L., and Kleuver, E. E., "An Assessment of Ground and Flight Simulators for the Examination of Manned Lunar Landing," AIAA Paper 1967-0238, Feb. 1967.

[8] Nassiff, S. H., and Armstrong, N. A., "Apollo Flightcrew Training in Lunar Landing Simulators," AIAA Paper 1968-254, March 1968.

[9] Jarvis, C. R., "Operational Experience with the Electronic Flight Control Systems of a Lunar-Landing Research Vehicle," NASA TN D-3689, Oct. 1966.

[10] Cheatham, D. C., and Hackler, C. T., "Handling Qualities for Pilot Control of Apollo Lunar-Landing Spacecraft," NASA TM X-57138,

Nov. 1964.
[11] Cheatham, D. C., and Moore, T. E., "Study of the Attitude Control Handling Qualities of the LEM During the Final Approach to Lunar Landing," NASA TM X-65228, May 1963.
[12] Hewes, D. E., "Interim Report on Flight Evaluations of Lunar Landing Vehicle Attitude Control Systems," AIAA Paper 1967-0239, Feb. 1967.
[13] Stengel, R. F., "Manual Attitude Control of the Lunar Module," *Journal of Spacecraft and Rockets*, Vol. 7, No. 8, Aug. 1970, pp. 941–948. doi:10.2514/3.30075
[14] Jarvis, C. R., "Flight-Test Evaluation of an on–off Rate Command Attitude Control System of a Manned Lunar-Landing Research Vehicle," NASA TN D-3903, April 1967.
[15] Cooper, G. E., "Understanding and Interpreting Pilot Opinion," *Aeronautical Engineering Review*, Vol. 16, No. 3, March 1957, pp. 47–51, 56.
[16] Jones, E. M., "The First Lunar Landing," *Apollo Lunar Surface Journal* [online database], http://history.nasa.gov/alsj/a11/a11.html [retrieved 4 Aug. 2009].
[17] Bilimoria, K. D., "Effects of Control Power and Guidance Cues on Lunar Lander Handling Qualities," *Journal of Spacecraft and Rockets*, Vol. 46, No. 6, Nov.–Dec. 2009, pp. 1261–1271. doi:10.2514/1.40187
[18] Cheatham, D. C., and Bennett, F. V., "Apollo Lunar Module Landing Strategy," *Apollo Lunar Landing Symposium*, NASA TM X-58006, June 1966, pp. 175–240.
[19] Hart, S. G., and Staveland, L. E., "Development of NASA-TLX (Task Load Index): Results of Empirical and Theoretical Research," *Human Mental Workload*, edited by P. A. Hancock, and N. Meshkati, North Holland Press, Amsterdam, 1988, pp. 239–350.
[20] Roscoe, A. H., and Ellis, G. A., "A Subjective Rating Scale for Assessing Pilot Workload in Flight: A Decade of Practical Use," Royal Aerospace Establishment TR 90019, Bedfordshire, England, U.K., March 1990.
[21] Rogers, W. F., "Apollo Experience Report: Lunar Module Landing Gear Subsystem," NASA TN D-6850, June 1972.
[22] Donahue, B. B., Caplin, G. N., and Smith, D. B., "Lunar Lander Concept Design for the 2019 NASA Outpost Mission," AIAA Paper 2007-6175, Sept. 2007.
[23] Shelton, D. H., "Apollo Experience Report—Guidance and Control Systems: Lunar Module Stabilization and Control System," NASA TN D-8086, Nov. 1975.
[24] Widnall, W. S., "Lunar Module Digital Autopilot," *Journal of Spacecraft and Rockets*, Vol. 8, No. 1, Jan. 1971, pp. 56–62. doi:10.2514/3.30217
[25] Veldman, A. E. P., Gerrits, J., Luppes, R., Helder, J. A., and Vreeburg, J. P. B., "The Numerical Simulation of Liquid Sloshing Onboard Spacecraft," *Journal of Computational Physics*, Vol. 224, No. 1, Jan. 2007, pp. 82–99. doi:10.1016/j.jcp.2006.12.020
[26] Shah, N., Hsu, O., and Garrick, J., "A Multibody Slosh Analysis for the Lunar Reconnaissance Orbiter," *AAS/GSFC Proceedings of the 20th International Symposium on Space Flight Dynamics*, NASA, Greenbelt, MD, Sept. 2007.
[27] "Modeling Fuel Slosh," ARES Corp., Rept. 451143110-003, Houston, TX, July 2007.
[28] Danek, G. L., "Vertical Motion Simulator Familiarization Guide," NASA TM 103923, May 1993.
[29] Aponso, B. L., Tran, D. T., and Schroeder, J. A., "Rotorcraft Research at the NASA Vertical Motion Simulator," AIAA Atmospheric Flight Mechanics Conference, AIAA Paper 2009-6056, 2009.
[30] Mueller, E. R., Bilimoria, K. D., and Frost, C. R., "Effects of Control Power and Inceptor Sensitivity on Lunar Lander Handling Qualities," AIAA Paper 2009-6407, Sept. 2009.
[31] Mueller, E. R., Bilimoria, K. D., and Frost, C., "Dynamic Coupling and Control Response Effects on Spacecraft Handling Qualities During Docking," *Journal of Spacecraft and Rockets*, Vol. 46, No. 6, Nov.–Dec. 2009, pp. 1288–1297. doi:10.2514/1.41924
[32] Penchuk, A., and Croopnick, S., "The Digital Autopilot for Thrust Vector Control of the Shuttle Orbital Maneuvering System," *Guidance and Control Conference*, San Diego, CA, AIAA Paper 1982-1579, Aug. 1982.

D. Spencer
Associate Editor